Journal of Membrane Science 348 (2010) 66–74

Contents lists available at ScienceDirect

Journal of Membrane Science

journal homepage: www.elsevier.com/locate/memsci

Influence of membrane properties on fouling in submerged membrane bioreactors

Perry van der Marel[a,b], Arie Zwijnenburg[b], Antoine Kemperman[a,*], Matthias Wessling[a], Hardy Temmink[b,c], Walter van der Meer[a,b]

[a] Membrane Technology Group, IMPACT Institute of Mechanics, Processes and Control Twente, Faculty of Science and Technology, University of Twente, P.O. Box 217, NL-7500 AE Enschede, The Netherlands
[b] Wetsus, Centre of Excellence for Sustainable Water Technology, P.O. Box 113, NL-8900 CC Leeuwarden, The Netherlands
[c] Department of Environmental Technology, Wageningen University, P.O. Box 8129, NL-6700 EV Wageningen, The Netherlands

ARTICLE INFO

Article history:
Received 19 February 2009
Received in revised form 16 October 2009
Accepted 23 October 2009
Available online 10 November 2009

Keywords:
Improved flux-step method
Critical flux and critical flux for irreversibility
Fouling reversibility
MBR

ABSTRACT

Polymeric flat-sheet membranes with different properties were used in filtration experiments with activated sludge from a pilot-scale MBR to investigate the influence of membrane pore size, surface porosity, pore morphology, and hydrophobicity on membrane fouling. An improved flux-step method was used to measure both the critical flux and critical flux for irreversibility. Long term experiments were performed to evaluate if influences of membrane properties on short term could be translated to long term fouling behavior.

The results showed that a hydrophilic asymmetric membrane with an interconnected pore structure, a nominal pore size of 0.3 μm, and large surface porosity of 27%, provided the best membrane performance with respect to critical flux and critical flux for irreversibility. The dominant fouling mechanism in long term filtration experiments was gel layer formation, which for this membrane was the least severe, and therefore extended the sustainable time.

1. Introduction

Membrane fouling of flat-sheet membranes in a submerged membrane bioreactor (sMBR) is caused by accumulation of feed water constituents on the surface of the membrane (cake and/or gel formation) or in the membrane matrix (pore blocking and/or adsorption). The nature and extent of the fouling is influenced by membrane properties [1], operational conditions (like aeration or the applied filtration protocol), and feed properties. The performance of different membranes in a sMBR can be examined using the critical flux concept [2], most commonly measured by flux-step methods [3–6]. The transmembrane pressure (TMP) increases with step-wise increase in flux, but remains stable during each flux-step below the critical flux. Previous work on critical flux-studies investigated the effect of membrane pore size and/or hydrophobicity. At the same time other membrane properties such as surface porosity, membrane material and pore morphology were varied (e.g. [7,8]). This makes a correlation with membrane fouling extremely difficult [9] and may have contributed to inconclusive results. For example, in different studies a larger pore size was shown to have no effect, a positive effect or a negative effect on the critical flux [6,10–13]. Clearly, the influence of membrane pore size on critical flux should be investigated in close relation to membrane surface porosity and pore morphology. In general membranes with larger pores also have larger surface porosities, resulting in a lower local flux [14,15] and lower transmembrane pressures (TMP), whereas pore morphology (pore structure and interconnectivity) affects the amount of internal fouling [16–18].

Intermediate physical cleaning (relaxation or backwashing) can help to remove some of the foulants, and in this manner restore filtration resistance [11]. This type of fouling is called reversible fouling. Applying physical cleaning in flux-step methods therefore enables to discriminate between reversible and irreversible fouling. In addition, a critical flux for irreversibility can be defined; i.e. the flux above which irreversible fouling occurs [4,19]. This critical flux for irreversibility equals the critical flux if all fouling is irreversible, while it exceeds the critical flux if fouling is (partially) reversible. The cleaning method that is applied should always be part of the definition of the critical flux for irreversibility. Cake layers generally can be removed by both relaxation and backwashing. On the other hand, internal fouling caused by pore blocking and adsorption, is hardly removed by these physical cleaning methods, and neither are gel layers (being more adhesive than a cake layer [20]) and compressed cake layers [21–23].

* Corresponding author. Tel.: [redacted]; fax: [redacted].
E-mail address: [redacted]@utwente.nl (A. Kemperman).

0376-7388/$ – see front matter © 2009 Elsevier B.V. All rights reserved.
doi:10.1016/j.memsci.2009.10.054

This study aimed at elucidating the influence of several membrane properties on membrane fouling. The influence of the pore size on the critical flux and critical flux for irreversibility were determined, taking into account differences in membrane material, hydrophobicity, surface porosity, and pore morphology. Long term experiments were performed to evaluate if influences of membrane properties on short term could be translated to long term fouling behavior.

2. Materials and methods

2.1. Membranes

To obtain membranes with different pore sizes, surface porosities, and pore morphologies four different polymeric membrane materials were selected from commercially available hydrophilic flat-sheet membranes (Table 1). Mixed cellulose ester (MCE) and polycarbonate (PC) membranes with four different pore sizes were obtained from filter discs (Ø 0.142 m) supplied by Millipore. Polyvinylidene fluoride membranes from Toray ($PVDF_T$) were obtained from flat-sheets previously used in a sMBR, and hydrophilised chlorinated polyethylene (PE) membranes from Kubota were obtained from commercially available A4 modules. Additionally, hydrophilic PVDF membranes with four different pore sizes were homemade using a diffusion induced phase inversion method by casting a PVDF dope solution on a polyester non-woven material and immersing it in a nonsolvent bath. By heat treatment one of the hydrophilic PVDF membranes was made hydrophobic afterwards ($PVDF_H$), without changing the other membrane properties.

2.2. Experimental MBR set-up

A lab-scale filtration set-up described in detail elsewhere was used [4]. Five reactors were used in parallel, and each reactor contained two vertically flat-sheet plates (Fig. 1). An aerator was placed below all membranes, providing a 0.4 $m^3\,h^{-1}$ air flow at approximately 0.25 $m\,s^{-1}$ superficial velocity across the membrane surface. Activated sludge circulated over the filtration set-up provided by a pilot-scale MBR of 85 L, which was fed with municipal wastewater [24]. The reactor volume and the hydraulic retention time in the filtration set-up were kept constant at 5 L and 1 h, respectively. The MBR operated at an average activated sludge concentration of $10 \pm 1.9\,g\,L^{-1}$.

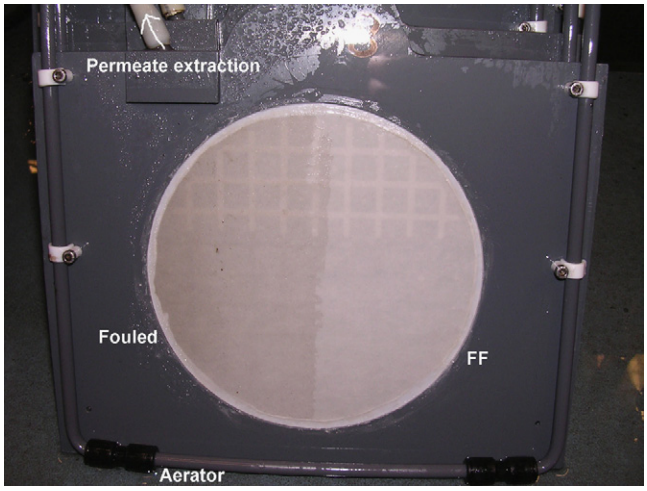

Fig. 1. Membrane-plate configuration.

Permeate was extracted and recycled to the filtration set-up. Labview software (National Instruments) was used to control the experiments and to store data. The hydraulic resistance (R) was calculated by Darcy's law (Eq. (1)). The TMP was calculated from absolute pressures measured with pressure sensors (Endress and Hauser, Cerabar M). The permeate flow was measured periodically to check the imposed flux (J). A temperature sensor measured the temperature (T in °C) of the activated sludge mixture, to allow correction of the dynamic viscosity of the permeate (η) for temperature [25]:

$$R = \frac{\mathrm{TMP}}{\eta J} \quad \text{with} \quad \eta = 0.497 \times (T + 42.5)^{-1.5} \tag{1}$$

2.3. Analytical methods

2.3.1. Membrane characterization

The nominal pore sizes of the membranes were obtained in three different ways: from supplier's specifications, by scanning

Table 1
Membrane properties.

Membrane		Nominal pore size			Contact angle (°)	Surface porosity (%)	Membrane thickness (μm)	Pore morphology	R_l (10^{10} m^{-1})
Material	Nr.	Specs (μm)	ImageJ (μm)	Bubblepoint (μm)					
PVDF	P1	n.a.	0.02	>0.05	71	4	65		20.5
	P2	n.a.	0.03	>0.05	69	6	110		9.8
	P3	n.a.	0.1	0.1	77	15	165	Asymmetric	4.3
	P4	n.a.	0.3	n.a.	n.a.	27	190		2.6
	H	n.a.	0.1	n.a.	101	15	165		5.4
PVDF	T	0.08	0.07	n.a.	84	7	320	Asymmetric	4.1
MCE	M1	0.1	0.1	0.1	71	23	100		26.1
	M2	0.5	0.8	0.6	[a]	31	150	Symmetric	0.8
	M3	3	1.8	1.7	[a]	37	150		0.3
	M4	8	2.7	3.3	[a]	41	135		<0.1
PE	K	0.4	0.3	0.3	[a]	25	165	Symmetric	4.6
PC	C1	0.1	0.1	0.07	n.a.	3	20		36.1
	C2	0.4	0.4	0.6	43	10	10	Straight capillaries	0.8
	C3	1.2	0.9	1.3	52	11	20		0.3
	C4	3	2.5	n.a.	n.a.	12	10		<0.1

n.a.: not available.
[a] The bubble changed significantly in time due to pore infiltration.

electron microscopy (SEM, JEOL-6480LV), and by bubble point analysis. SEM pictures of the membrane surface were analyzed with image processing software to determine the nominal pore size and the surface porosity (ImageJ, NiH). SEM pictures of membrane cross-sections were analyzed visually to obtain pore morphology and membrane thickness. Bubble point analysis was performed by a Coulter porometer II (wetting fluid, trade name 'Porofil'). Hydrophobicity of the membranes was measured by a contact angle measurement with a CAM-200 (KSV). The contact angle of a droplet of Milli-Q ultrapure water (3 μL) after 30 s was reported.

2.3.2. Examining membrane fouling: improved flux-step method and long term experiments

For each membrane three experiments were carried out, each consisting of 10 consecutive runs of an improved flux-step method (IFSM [4]), to determine an average critical flux and critical flux for irreversibility. Each run in the IFSM consisted of incrementing flux-steps of 5 L m^{-2} h^{-1} from 5 to 100 L m^{-2} h^{-1} in steps, with an intermediate relaxation step at a low reference flux of 5 L m^{-2} h^{-1}. Five hours of relaxation were applied in between each distinct consecutive run, resulting in 15 h total time per run (10 h for the IFSM run and 5 h for the relaxation period). The initial filtration resistance (R_I) was determined in each consecutive filtration run as the average for the first 6 flux-steps (i.e. below the critical flux). This value for the first run equaled the clean membrane resistance, and an increase with consecutive runs gave an indication for the occurrence of irreversible fouling.

Long term experiments were performed at a fixed flux with or without intermediate relaxation. In the case of relaxation, two filtration protocols were applied to obtain two different net fluxes; i.e. the instantaneous flux corrected for the loss of permeate during the intermediate relaxation. Filtration for 8 min at a flux of 32 L m^{-2} h^{-1} followed by 2 min relaxation resulted in a net flux of 25 L m^{-2} h^{-1}, arbitrarily chosen as being a standard operating flux for full-scale submerged flat-sheet MBRs. Furthermore filtration for 15 min at a flux of 100 L m^{-2} h^{-1} followed by 15 min relaxation resulted in a net flux of 50 L m^{-2} h^{-1}. The end-resistance is given just before applying relaxation.

2.4. Membrane cleaning

The membranes were physically and chemically cleaned only after experiments were finished. First, the flat-sheet membranes were removed from the membrane tank. Physical cleaning was applied with a water jet running at 0.5 L min^{-1} at 5×10^4 Pa (called a forward flush, FF), removing all accumulated feed water constituents from the surface of the membrane (also see Fig. 1). Chemical cleaning was applied by soaking the membrane for 2 h in 2000 ppm sodium hypochlorite (NaOCl).

2.5. Chemical oxygen demand

The chemical oxygen demand (COD) of permeate of the membranes with different nominal pore sizes was measured with photometric test kits (Dr. Lange, Hach, Merck).

3. Results

3.1. Membrane characterization

Table 1 shows the membrane properties. For every series of membranes from the same supplier the surface porosity increased with increasing pore size. Additional bubble point analyses were performed since the MCE pore sizes provided by the supplier did not agree with those from the ImageJ analyses. For each membrane the pore size determined with the ImageJ analysis is used throughout this chapter to refer to the membrane examined. For the larger pores contact angle measurement revealed pore infiltration by the bubbles. Nevertheless, it was concluded that all membranes were hydrophilic, except for the hydrophobized PVDF membrane ($PVDF_H$).

SEM images of the feed side surfaces (Fig. 2A) and cross-sections (Fig. 2B) revealed distinct differences in pore morphologies of the different membrane materials. The pore structure either showed an increasing pore size from the skin towards the permeate side (asymmetric structure or surface filter for PVDF membranes) or an

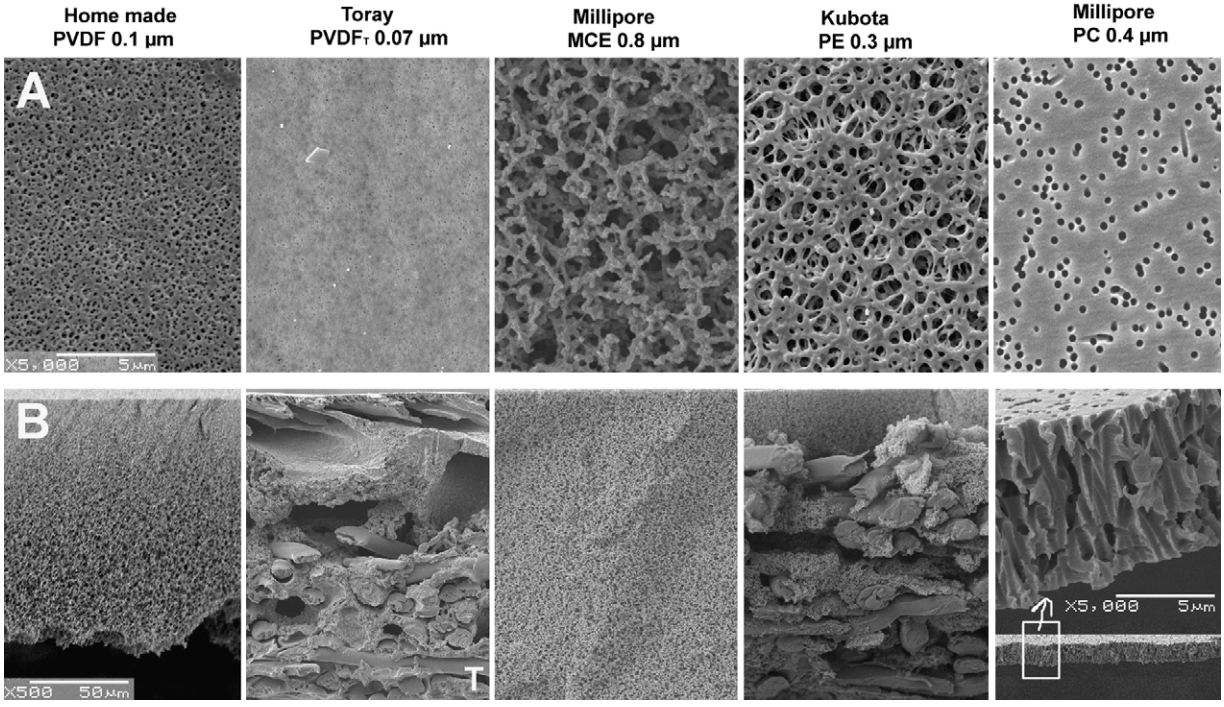

Fig. 2. SEM images of the feed side of five different membrane materials (A, 5000×) and their cross-sections with filtration direction from top to bottom (B, 500×).

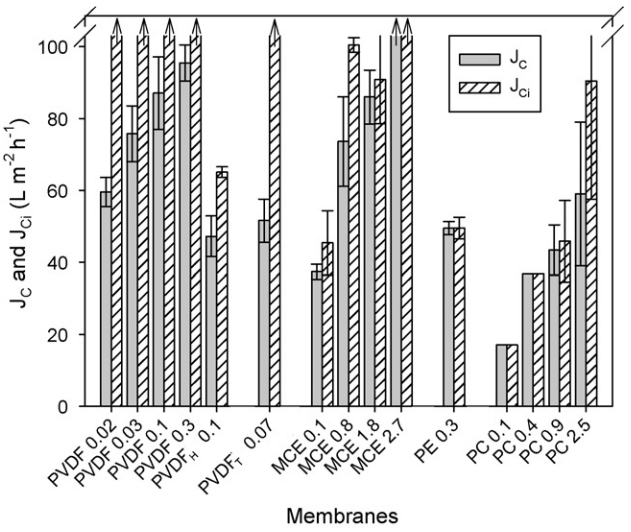

Fig. 3. Critical flux (J_C) and critical flux for irreversibility (J_{Ci}) for different membranes. These parameters are averaged for three experiments (error bars indicated) and for only the first out of 10 consecutive runs of the improved flux-step method. The upwards arrow indicates a parameter value larger than the used maximum flux. The numbers on the *x*-axis are the membrane pore sizes in μm as determined by SEM ImageJ analysis.

uniform pore size over the cross-section (symmetric structure or depth filter for PE and MCE membranes). The homemade PVDF, PE, and MCE membranes had an interconnected pore morphology. The PC membranes consisted of straight-through pores without interconnectivity, whereas the Toray membrane ($PVDF_T$) consisted of a thin dense skin (<1 μm) on a substructure with large macro-voids. Table 1 also shows that the membrane resistance decreased with increasing pore size and/or surface porosity.

3.2. Critical flux (J_C) and critical flux for irreversibility (J_{Ci})

Fig. 3 shows the critical flux and critical flux for irreversibility for the different membranes (average value of three experiments; values taken from the first run of the 10 consecutive IFSM runs). Membranes PC 0.1 μm and PC 0.4 μm were only measured once because of severe fouling during the experiments. The upwards arrow (↑) indicates when the critical fluxes exceeded the maximum flux of 100 L m^{-2} h^{-1} that was applied in the IFSM method. Clear differences were observed, which will be discussed below.

3.2.1. Pore size and surface porosity

The critical flux increased with increasing pore size and/or surface porosity. This may be explained by a lower local flux through the pores and a smaller retention of feed water constituents. The lower retention for membranes with larger pore sizes was verified from permeate COD values, which increased by 3% from PVDF 0.02 μm to PVDF 0.3 μm, 11% from MCE 0.1 μm to MCE 2.7 μm, and 14% from PC 0.1 to PC 2.5 μm.

3.2.2. Hydrophobicity and membrane material

Hydrophobic membrane $PVDF_H$ 0.1 μm showed approximately half the critical flux compared to the hydrophilic membrane PVDF 0.1 μm, although all the other membrane properties were the same. The lower critical flux is explained by a faster adsorption of feed water constituents on membrane $PVDF_H$ 0.1 μm. Consequently, the pores narrow for membrane $PVDF_H$ 0.1 μm, yielding a lower critical flux. This also explained the larger retention of feed constituents by membrane $PVDF_H$ 0.1 μm, indicated by a 5% lower permeate COD despite a similar pore size compared to membrane PVDF 0.1 μm. Adsorption is irreversible by relaxation and therefore explained the critical flux for irreversibility being a fraction larger than the critical flux.

The higher critical flux for membrane PVDF 0.03 μm compared to membrane $PVDF_T$ 0.07 μm was surprising since both are made of PVDF (additives undisclosed), and membrane $PVDF_T$ 0.07 μm had a larger pore size and similar surface porosity. Membrane $PVDF_T$ 0.07 μm therefore unexpectedly gave a lower critical flux for which no explanation can be given at this time.

3.2.3. Pore morphology

Differences in pore morphology may explain differences in critical fluxes for irreversibility for (1) the PVDF, MCE, and PC membranes and (2) the lower critical flux and critical flux for irreversibility of membrane PE 0.3 μm compared to membrane PVDF 0.3 μm.

The homemade PVDF membranes exhibited a critical flux for irreversibility which exceeded the critical flux, indicating that the fouling was reversible during the relaxation step. From SEM observations no adsorption could be observed and it was assumed that all material entering the membrane could also flow out with the permeate, due to the asymmetric pore morphology of these membranes. A similar observation was made for membrane $PVDF_T$ 0.07 μm.

MCE membranes are depth filters and particle entrapment occurred along the tortuous path in the membrane matrix (SEM). This type of morphology may be responsible for the faster irreversible fouling and consequently lower values of critical flux and critical flux for irreversibility of MCE membranes compared to homemade PVDF membranes. The increase in critical flux with increasing pore size for the MCE membranes can be explained by the higher volume porosity which was 73% for MCE 0.1 μm, 79% for MCE 0.8 μm, 83% for MCE 1.8 μm, and 84% for MCE 2.7 μm (data of the membrane supplier). Membrane PE 0.3 μm exhibited a critical flux for irreversibility which was similar to its critical flux. This can also be attributed to pore blocking of the symmetric pore morphology (depth filter). Its difference with the asymmetric membrane PVDF 0.3 μm was remarkable in view of equal pore size and surface porosity. Pore filling did not occur for membrane PVDF 0.3 μm, explaining the larger critical flux and critical flux for irreversibility compared to membrane PE 0.3 μm.

The four PC membranes also incurred irreversible fouling, which could be explained by pore blocking elucidated by SEM investigation. The much lower critical fluxes compared to homemade PVDF membranes can be explained by the differences in pore morphology. Ho and Zydney [17] showed that membranes with an interconnected pore structure fouled more slowly compared to membranes with track-etched straight capillaries. In an interconnected pore structure the permeate can by-pass blocked pores via the interconnections, which is not possible for straight-through track-etched pores. Consequently, membranes with straight-through pores have a lower critical flux. A large standard deviation was measured for membranes PC 0.9 μm and PC 2.5 μm. Sludge particles passed the membrane pores for these membranes, and were entrapped in between the non-woven and the membrane. These particles were supposed to flow through the non-woven having much larger pores. Its unexpected retention by the non-woven occurred randomly with increasing flux, affecting accurate fouling (reversibility) measurements.

3.3. Irreversible fouling during consecutive filtration runs

Fig. 4 shows the development of initial membrane resistances (R_I) for 11 different membranes during 10 consecutive IFSM runs (note the different scales on the *y*-axes). Fouling for the PC membranes was too severe to perform a second consecutive run and therefore is not included in Fig. 4. An increase in initial membrane

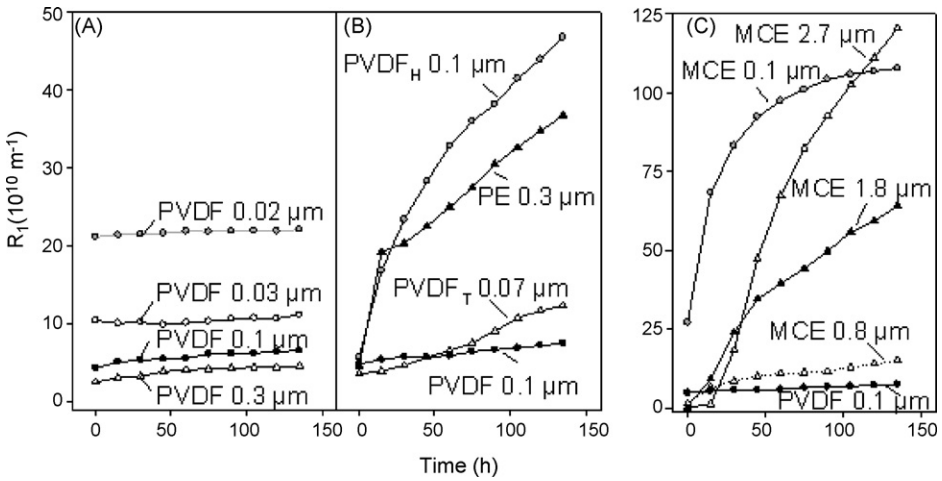

Fig. 4. Initial membrane resistance (R_1) during 10 consecutive runs for 11 membranes; P3 is shown in each graph for easy comparison (notice the identical *y*-axis scale for 5A and 5B, and the larger *y*-axis scale for 5C).

resistance during 10 consecutive runs is an indication for the occurrence of irreversible fouling.

The initial membrane resistance remained fairly stable during 150 h for the homemade PVDF membranes (Fig. 4A). No significant irreversible fouling occurred during the 10 runs and the critical fluxes remained constant (not shown). Irreversible fouling in each distinct run occurred for membranes PVDF$_H$ 0.1 µm, PVDF$_T$ 0.07 µm, and PE 0.3 µm shown by the increase in initial filtration resistance (Fig. 4B). All three membranes however, did not show a significant change in critical flux in the consecutive runs. This was surprising, as it was expected that irreversible fouling would increase the local flux (narrow pores and reduces the surface porosity), and in this manner also would decrease the critical flux.

The continuous increase in initial resistance for hydrophobic membrane PVDF$_H$ 0.1 µm contradicted with the nearly constant initial resistance for membrane PVDF 0.1 µm having the same membrane properties but a more hydrophilic character. Such behavior clearly complies with the aforementioned larger irreversible fouling tendency of membrane PVDF$_H$ 0.1 µm attributed to adsorption. Membrane PE 0.3 µm exhibited a fast increase in initial membrane resistance between run 1 and run 2, followed by a more moderate increase. A partially blocked pore matrix was the cause of this increase elucidated by SEM observations of membrane PE 0.3 µm after 10 consecutive runs (Fig. 5). Membrane PVDF$_T$ 0.07 µm showed a very small but gradual increase in initial filtration resistance, which did not result in a critical flux for irreversibility below 100 L m^{-2} h^{-1}. Visual observation showed that membrane PVDF$_T$ 0.07 µm had changed in color from white to brown after 10 filtration runs. This was attributed to adsorption, also explaining the increase in membrane resistance.

Severe particle entrapment for depth filter MCE membranes occurred when the value of the critical flux was exceeded in each of the 10 runs, shown by the drastic increase in initial membrane resistance (Fig. 4C). This increase in resistance was more severe for the MCE membranes compared to membrane PE 0.3 µm, in spite of similar symmetric pore morphology, indicating larger volume porosity for the MCE membranes. Membrane MCE 2.7 µm showed the largest increase in resistance, which can be attributed to the largest volume porosity (Fig. 5). Open depth filters apparently only initially have a good membrane performance, considering the superior critical fluxes as determined in the first run of the IFSM for membrane MCE 2.7 µm (see Section 3.2.3). The critical flux for MCE 2.7 µm dropped to 31 L m^{-2} h^{-1} for membrane MCE 2.7 µm but only to 60 L m^{-2} h^{-1} for membrane MCE 0.8 µm. For unknown reasons MCE 0.8 µm membrane had a remarkable good membrane performance compared to the other three MCE membranes, as shown by the much lower increase in initial membrane resistance.

3.4. Long term experiments

3.4.1. Sub-critical filtration with homemade PVDF membranes at fixed flux

Sub-critical filtration at a fixed flux of 50 L m^{-2} h^{-1} was performed with the homemade PVDF 0.03 µm, PVDF 0.1 µm, and PVDF 0.3 µm membranes to investigate the influence of pore size and surface porosity (6, 15, and 27%, respectively) on long term fouling behavior (Fig. 6). A characteristic two-stage resistance profile [15,20,26,27] was observed for PVDF 0.03 µm and PVDF 0.1 µm. PVDF 0.3 µm showed a stable filtration resistance for more than 300 h. The gradual rise in resistance in the first stage can be explained by irreversible fouling: adsorption, pore blocking, and/or local deposition on the membrane of macromolecules, like extracellular polymeric substances (EPS [28]). These fouling mechanisms blocked part of the membrane, progressively increasing the local flux. The duration of the first stage is called the sustainable time [26], which clearly increased with increasing pore size and/or surface porosity. The rapid increase for PVDF 0.03 µm and PVDF 0.1 µm in Fig. 6 was caused by the gel layer formation detected on the fouled membranes (see Fig. 1, darker part of the membrane).

3.4.2. Long term filterability with commercial membranes

The long term fouling behavior of membrane PVDF 0.1 µm was compared to commercial membranes PE 0.3 µm and PVDF$_T$ 0.07 µm. The latter two membranes where selected in this experiment for practical relevance. The results are shown in Fig. 7. Filtration started at a fixed flux of 25 L m^{-2} h^{-1}, and the flux was gradually step-wise increased after 140 h to speed up the fouling process.

The resistance initially increased faster for membrane PE 0.3 µm compared to membranes PVDF$_T$ 0.07 µm and PVDF 0.1 µm, probably due to pore blocking, similar to the results shown in Fig. 4. Incrementing the flux also showed a two-stage fouling process. Although membrane PE 0.3 µm and membrane PVDF$_T$ 0.07 µm approximately had the same critical flux, with membrane PE 0.3 µm a shorter sustainable time was achieved. Membranes PVDF$_T$ 0.07 µm and PE 0.3 µm both showed a gel layer on the membrane surface at the end of the experiment. Membrane PVDF 0.1 µm only showed a gradual increase in resistance upon increasing the flux, while gel formation did not occur.

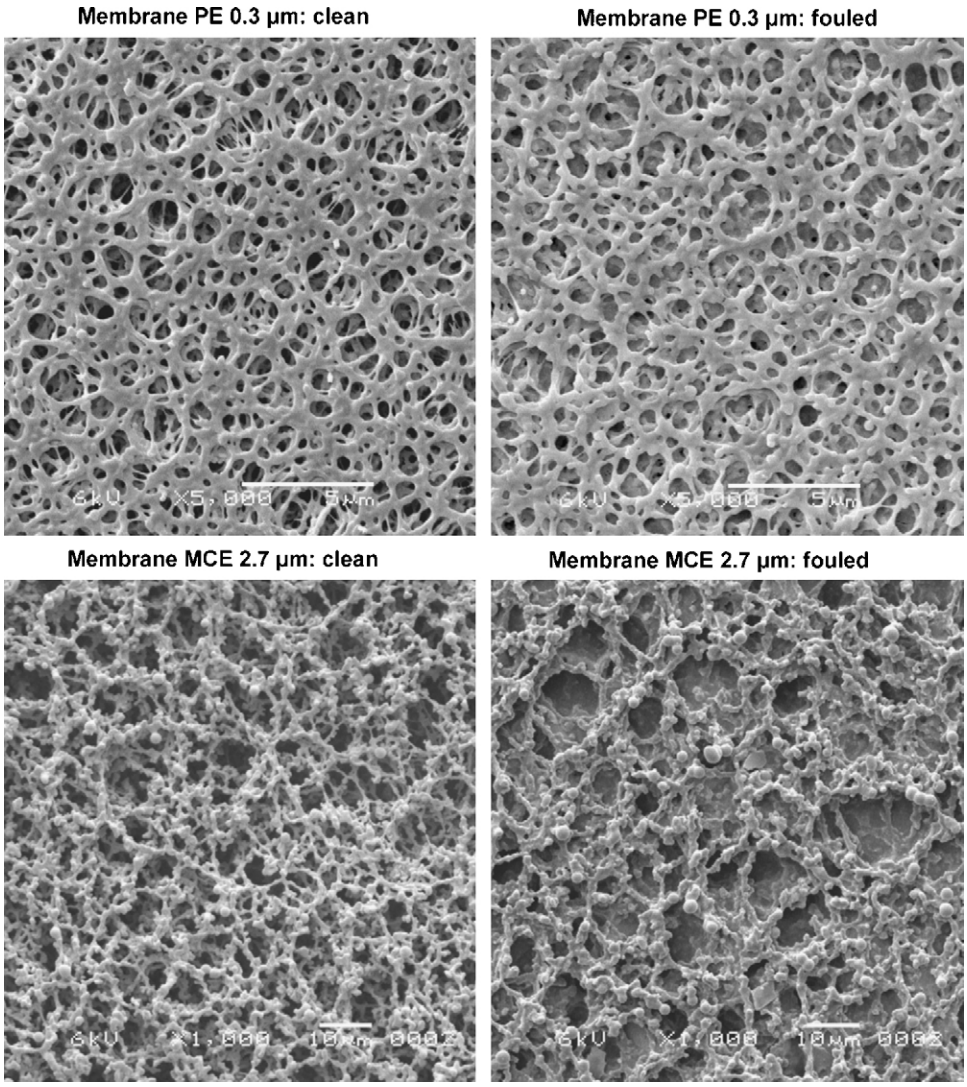

Fig. 5. Membranes PE 0.3 μm (5000×, top) and MCE 2.7 μm (1000×, bottom) clean and fouled after 10 consecutive runs.

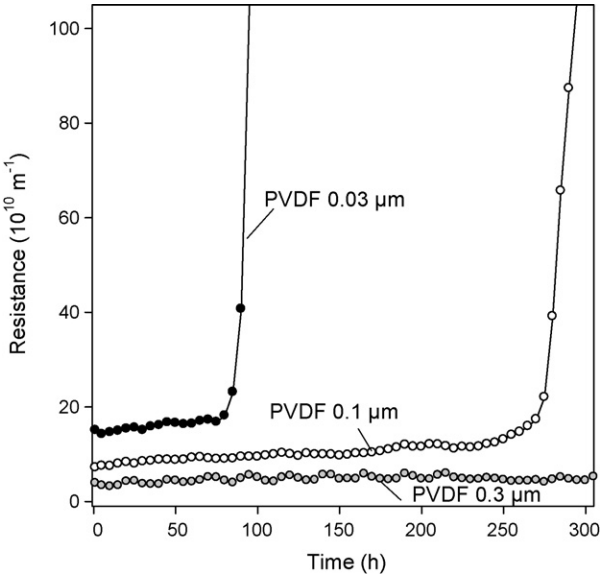

Fig. 6. Filtration resistance of PVDF 0.03 μm, PVDF 0.1 μm and PVDF 0.3 μm during fixed flux filtration at a flux of 50 L m^{-2} h^{-1}.

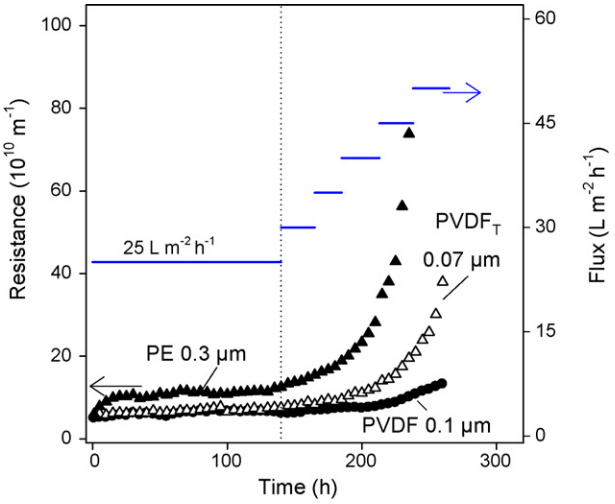

Fig. 7. Filtration resistance of PVDF 0.1 μm, PE 0.3 μm, and PVDF$_T$ 0.07 μm at incrementing fixed flux from 25 to 50 L m^{-2} h^{-1}.

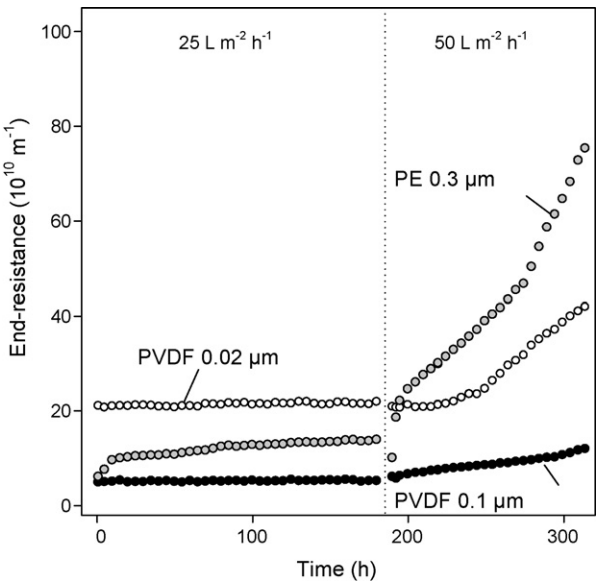

Fig. 8. End-resistances of PVDF 0.02 μm, PVDF 0.1 μm, and PE 0.3 μm at two net fluxes, with intermittent relaxation (after 8 min filtration at 32 L m^{-2} h^{-1} 2 min relaxation resulting in a net flux of 25 L m^{-2} h^{-1}, or after 15 min at 100 L m^{-2} h^{-1} for 15 min relaxation resulting in a net flux of 50 L m^{-2} h^{-1}).

3.4.3. Fouling behavior with intermittent relaxation at two different net fluxes

In full-scale installations, submerged flat-sheet membranes are operated with intermittent relaxation, which might affect the fouling behavior of different membranes. For this reason, long term filtration with intermittent relaxation at two different net fluxes was performed for membranes PVDF 0.02 μm, PVDF 0.1 μm, and PE 0.3 μm (Fig. 8). Initially, the net flux was 25 L m^{-2} h^{-1}, by operating for 8 min at a flux of 32 L m^{-2} h^{-1} followed by 2 min relaxation. After chemical cleaning, a twice as high net flux was applied by 15 min of filtration at 100 L m^{-2} h^{-1} followed by 15 min of relaxation.

At a net flux of 25 L m^{-2} h^{-1} no differences were observed in the development of the end-resistance for membranes PVDF 0.1 μm and PE 0.3 μm compared to the resistance development during fixed flux operation at the same flux value (see Fig. 7). Relaxation therefore did not affect the fouling behavior at these sub-critical conditions intermediate. Increasing the net flux to 50 L m^{-2} h^{-1} resulted in unsustainable membrane performance for membrane PE 0.3 μm. The instantaneous flux of 100 L m^{-2} h^{-1} was far above the critical flux of 49 L m^{-2} h^{-1}. The fast initial increase in end-resistance was explained by initial pore blocking, and shortly after start-up gel layer formation occurred. Cake layer formation clearly was absent, most likely because a cake layer has a higher reversibility by intermittent relaxation than a gel layer. The instantaneous flux also was above the critical flux for membrane PVDF 0.02 μm (75 L m^{-2} h^{-1}) but a sustainable filtration still was possible for 48 h at the net flux of 50 L m^{-2} h^{-1}. With membrane PVDF 0.1 μm only a gradual increase in resistance was detected, although sooner or later this probably also may have lead to a rapid increase in resistance. The differences in membrane behavior clearly demonstrate the importance of membrane pore size and surface porosity (membranes PVDF 0.02 μm and PVDF 0.1 μm), and pore morphology (membranes PVDF 0.1 μm and PE 0.3 μm) on gel layer formation and membrane performance.

4. Discussion

The experiments described in this paper focused on understanding the influence of membrane properties on membrane fouling in MBRs. The results clearly demonstrated that membrane material, pore size, surface porosity, pore morphology, and hydrophobicity all have a strong effect on membrane fouling.

Different polymeric materials cause different degrees of adsorption [29,30]. Adsorption was also different for membranes PVDF 0.03 μm and PVDF$_T$ 0.07 μm which were both made of the organic polymer PVDF (additives undisclosed for membrane PVDF$_T$ 0.07 μm). Membrane PVDF$_T$ 0.07 μm discolored from initially white to brown during filtration caused by adsorption, whereas membrane PVDF 0.03 μm did not change in color. This difference in adsorption seemed the most likely cause of the difference in critical flux between membrane PVDF$_T$ 0.07 μm and membrane PVDF 0.03 μm. The different adsorption behavior can be caused by the more hydrophobic character of membrane PVDF$_T$ 0.07 μm (Table 1). The surface charge, the surface roughness, or the different dope components also may have caused the difference in adsorption, which properties however were beyond the scope of this investigation.

Membranes with larger pores often also have a larger surface porosity. Unfortunately it is very difficult to obtain membranes with identical surface porosities but different pore sizes or vice versa, which makes it hard to uncouple the effects of pore size and surface porosity on fouling behavior. This study showed that increasing pore size and surface porosity reduces membrane fouling (larger critical flux) explained by a lower local flux through the pores and a smaller retention of feed water constituents. A higher surface porosity lowers the local flux to and through each pore, thus decreasing the drag force of material towards the membrane and increasing the critical flux. At similar fluxes a reduced retention reduces concentration polarization, allowing a higher flux before concentration polarization results in cake or gel formation [23]. Other studies suggested more internal fouling for larger pore membranes, as more material can pass the membrane skin and become entrapped in the membrane matrix [31,32]. We showed this only applies for membranes with a symmetric pore morphology. Internal fouling is mitigated in asymmetric membranes; i.e. constituents smaller than the pore size entering the membrane matrix can leave with the permeate flow.

The MCE membranes showed a larger critical flux with increasing pore size, i.e. with increasing volume porosity. A larger volume porosity implies a larger dirt-loading capacity being able to entrap more material in the pore matrix which mitigates fouling. On the longer term (consecutive filtration runs, Fig. 4) however, the MCE membrane with the largest pore (MCE 2.7 μm) clearly was more severely fouled. A larger volume porosity for depth filters therefore is only beneficial on short term filtration. Membrane MCE 0.8 μm revealed a remarkably good behavior on long term filtration. A reason could be that the feed mixture contained a much lower concentration of fouling constituents in the pore size range of MCE 0.8 μm. This behavior can also explain the relatively large critical flux for irreversibility of membrane MCE 0.8 μm compared to membrane MCE 1.8 μm (Fig. 3).

The influence of membrane hydrophobicity on membrane fouling often is determined by comparing membranes not only different in their hydrophobic nature but also in other properties. In this study, it was possible to only vary hydrophobicity. From this it was demonstrated that the critical flux for a hydrophobic membrane PVDF$_H$ 0.1 μm only was half of that of a hydrophilic membrane PVDF 0.1 μm. The primarily hydrophobic nature of the biomass [33] was believed to cause a faster adsorption of feed water constituents on membrane PVDF$_H$ 0.1 μm.

A study by Choi and Ng [34] indicated that hydrophobicity only affects fouling in the initial state by adsorption, where after these surface characteristics are masked by the adsorption layer. Our results however showed that hydrophobicity results in progressive fouling during consecutive filtration runs, for which the mechanism

was not clearly identified. Adsorption occurred by a multi-layer process and/or a transparent gel layer could have caused the progressive fouling, i.e. visual observation after the experiment did not show a deposit like that in Fig. 1. A gel layer as the cause is supported by previous studies [14,35–37] showing that hydrophobic membranes are less resistant to fouling by EPS.

An increase in net flux above fluxes conventionally applied in full-scale installations is of interest since it would imply that a smaller membrane surface area can be installed. This also reduces energy consumption by air scouring, which is the main cost for submerged units and can contribute to more than 90% of the total costs [38]. For instance, Fig. 8 shows that the net flux for asymmetric membrane PVDF 0.1 μm can be approximately twice as high as that for symmetric membrane PE 0.3 μm. The long term experiments showed that membranes with a larger critical flux and critical flux for irreversibility also can be operated at a larger net flux, and/or shows a longer sustainable time at similar instantaneous fluxes.

Ognier et al. [15] and Cho and Fane [27] explained the rapid increase in resistance, for example those in Fig. 6, by the gradual increase in local flux eventually exceeding the critical flux, causing severe cake layer formation. Visual observation of the membranes in our study clearly did not show cake layer formation but gel layer formation as the source of the rapid increase in resistance, complying with findings in a recent study by Wang et al. [20]. It is hypothesized that the gradual increase in local flux also increases concentration polarization, and the transition to gel formation occurred when the gel concentration [39] of the macromolecular species present was reached. Subsequently, a gel was formed which became thicker or more compact due to the ongoing convection of material to the membrane, explaining the rapid rise in resistance.

The longer sustainable time for membrane PVDF 0.3 μm compared to membrane PVDF 0.03 μm and PVDF 0.1 μm (Fig. 6) can be explained by its lower local flux and lower retention; i.e. larger critical flux, both avoiding gel layer formation in this experiment. The shorter sustainable time for membrane PE 0.3 μm compared to membrane PVDF 0.1 μm in Fig. 7 can be explained by the more severe irreversible fouling for membrane PE 0.3 μm. This irreversible fouling caused a faster rise in local flux for membrane PE 0.3 μm compared to membrane PVDF 0.1 μm, consequently causing gel layer formation to occur sooner on the partially blocked pore matrix despite the larger pore size and surface porosity.

It is gel layer formation that hampers sustainable filtration on the long term (both at sub and supra-critical conditions). Future research therefore should focus on tackling gel layer formation by elucidating gel layer composition, and investigating the processes that contribute to the characteristics two-stage fouling process. Together with selection of appropriate membranes properties, this may lead to much higher sustainable fluxes. Finally, it cannot be ignored that the effect of membrane properties on membrane fouling also is determined by the feed properties. A future study therefore also will compare membranes with similar properties, but while using various sources of activated sludge.

5. Conclusion

The results of the improved flux-step method and the long term experiments showed a clear influence of the membrane properties on membrane fouling in a submerged membrane bioreactor. A hydrophilic membrane with a complete asymmetric, interconnected pore morphology, a relatively large pore size of 0.3 μm and a surface porosity of 27%, resulted in the best membrane performance.

By using the best performing membranes, much larger fluxes can be applied in a sustainable manner, or at similar fluxes can result in a longer sustainable time. Long term sustainable filtration eventually is hampered by gel layer formation which should be the topic of future research.

List of abbreviations

COD	chemical oxygen demand ($mg\,L^{-1}$)
EPS	extracellular polymeric substances
FF	forward flush
IFSM	improved flux-step method
J	flux ($L\,m^{-2}\,h^{-1}$)
J_C	critical flux ($L\,m^{-2}\,h^{-1}$)
J_{Ci}	critical flux for irreversibility ($L\,m^{-2}\,h^{-1}$)
η	permeate viscosity (Pa s)
R_I	initial membrane resistance (m^{-1})
R_{end}	end-resistance measured before relaxation is applied (m^{-1})
sMBR	submerged membrane bioreactor
TMP	transmembrane pressure (Pa)

Acknowledgements

This work was performed in the TTIW-cooperation framework of Wetsus, Centre of Excellence for Sustainable Water Technology (www.wetsus.nl). Wetsus is funded by the Dutch Ministry of Economic Affairs, the European Union Regional Development Fund, the Province of Fryslân, the City of Leeuwarden and the EZ/Kompas program of the 'Samenwerkingsverband Noord-Nederland'. The authors like to thank the participants of the research theme 'Membrane Bioreactors' for the discussions and their financial support. The company DSM is acknowledged in particular for their contribution in the contact angle measurements.

Kubota, Toray, and Millipore are acknowledged for supplying the flat-sheet membranes. Norit is acknowledged for providing the PVDF dope solution to prepare our homemade PVDF membranes.

References

[1] I.S. Chang, et al., Membrane fouling in membrane bioreactors for wastewater treatment, Journal of Environmental Engineering 128 (2002) 1018–1029.
[2] R.W. Field, et al., Critical flux concept for microfiltration fouling, Journal of Membrane Science 100 (1995) 259–272.
[3] P. Le Clech, et al., Critical flux determination by the flux-step method in a submerged membrane bioreactor, Journal of Membrane Science 227 (2003) 81–93.
[4] P. van der Marel, et al., An improved flux-step method to determine the critical flux and critical flux for irreversibility in a membrane bioreactor, Journal of Membrane Science 332 (2009) 24–29.
[5] G. Andreottola, G. Guglielmi, Critical flux determination in two MBRs for municipal wastewater treatment, in: Proceedings of the IMSTEC, Sydney, Australia, 2003.
[6] S.S. Madaeni, A.G. Fane, D.E. Wiley, Factors influencing critical flux in membrane filtration of activated sludge, Journal of Chemical Technology and Biotechnology 74 (1999) 539–543.
[7] S. Metsamuuronen, J. Howell, M. Nystrom, Critical flux in ultrafiltration of myoglobin and baker's yeast, Journal of Membrane Science 196 (2002) 13–25.
[8] Z. Wu, et al., Effects of various factors on critical flux in submerged membrane bioreactors for municipal wastewater treatment, Separation and Purification Technology 62 (2008) 56–63.
[9] P. Le-Clech, V. Chen, T.A.G. Fane, Fouling in membrane bioreactors used in wastewater treatment, Journal of Membrane Science 284 (2006) 17–53.
[10] D.Y. Kwon, et al., Experimental determination of critical flux in cross-flow microfiltration, Separation and Purification Technology 19 (2000) 169–181.
[11] S.J. Judd, The MBR Book: Principles and Applications of Membrane Bioreactors in Water and Wastewater Treatment, 1st ed., Elsevier, Oxford, 2006.
[12] D. Wu, J.A. Howell, R.W. Field, Critical flux measurement for model colloids, Journal of Membrane Science 152 (1999) 89–98.
[13] V. Chen, Performance of partially permeable microfiltration membranes under low fouling conditions, Journal of Membrane Science 147 (1998) 265–278.
[14] A.G. Fane, C.J.D. Fell, A review of fouling and fouling control in ultrafiltration, Desalination 62 (1987) 117–136.
[15] S. Ognier, C. Wisniewski, A. Grasmick, Membrane bioreactor fouling in subcritical filtration conditions: a local critical flux concept, Journal of Membrane Science 229 (2004) 171–177.
[16] Q.L. Wu, B.M. Wu, Study of membrane morphology by image-analysis of electron-micrographs, Journal of Membrane Science 105 (1995) 113–120.

[17] C.C. Ho, A.L. Zydney, Effect of membrane morphology on the initial rate of protein fouling during microfiltration, Journal of Membrane Science 155 (1999) 261–275.
[18] H.H.P. Fang, X. Shi, Pore fouling of microfiltration membranes by activated sludge, Journal of Membrane Science 264 (2005) 161–166.
[19] B. Espinasse, P. Bacchin, P. Aimar, On an experimental method to measure critical flux in ultrafiltration, Desalination 146 (2002) 91–96.
[20] Z. Wang, et al., Membrane fouling in a submerged membrane bioreactor (MBR) under sub-critical flux operation: membrane foulant and gel layer characterization, Journal of Membrane Science 325 (2008) 238–244.
[21] L. Defrance, M.Y. Jaffrin, Reversibility of fouling formed in activated sludge filtration, Journal of Membrane Science 157 (1999) 73–84.
[22] Y.K. Benkahla, et al., Cake growth-mechanism in cross-flow microfiltration of mineral suspensions, Journal of Membrane Science 98 (1995) 107–117.
[23] V. Chen, et al., Particle deposition during membrane filtration of colloids: transition between concentration polarization and cake formation, Journal of Membrane Science 125 (1997) 109–122.
[24] M. Remy, et al., Low dose powdered activated carbon addition at high sludge retention times to reduce fouling in membrane bioreactors, Water Research 43 (2009) 345–350.
[25] J.H. Roorda, J. van der Graaf, New parameter for monitoring fouling during ultrafiltration of WWTP effluent, Water Science and Technology 43 (2001) 241–248.
[26] G. Guglielmi, et al., Sub-critical fouling in a membrane bioreactor for municipal wastewater treatment: experimental investigation and mathematical modelling, Water Research 41 (2007) 3903–3914.
[27] B.D. Cho, A.G. Fane, Fouling transients in nominally sub-critical flux operation of a membrane bioreactor, Journal of Membrane Science 209 (2002) 391–403.
[28] A. Drews, C.-H. Lee, M. Kraume, Membrane fouling—a review on the role of EPS, Desalination 200 (2006) 186–188.
[29] N. Yamato, et al., Difference in membrane fouling in membrane bioreactors (MBRs) caused by membrane polymer materials, Journal of Membrane Science 280 (2006) 911–919.
[30] G. Zhang, et al., Adsorptive fouling of extracellular polymeric substances with polymeric ultrafiltration membranes, Journal of Membrane Science 309 (2008) 28–35.
[31] E.S. Tarleton, R.J. Wakeman, Understanding flux decline in cross-flow microfiltration. 1. Effects of particle and pore-size, Chemical Engineering Research & Design 71 (1993) 399–410.
[32] G. Gesan-Guiziou, R.J. Wakeman, G. Daufin, Stability of latex crossflow filtration: cake properties and critical conditions of deposition, Chemical Engineering Journal 85 (2002) 27–34.
[33] I.S. Chang, S.O. Bag, C.H. Lee, Effects of membrane fouling on solute rejection during membrane filtration of activated sludge, Process Biochemistry 36 (2001) 855–860.
[34] J.-H. Choi, H.Y. Ng, Influence of membrane material on performance of a submerged membrane bioreactor, in: Vol. Proceedings IWA conference Harrogate, 2007.
[35] A.D. Marshall, P.A. Munro, G. Tragardh, The effect of protein fouling in microfiltration and ultrafiltration on permeate flux, protein retention and selectivity—a literature review, Desalination 91 (1993) 65–108.
[36] S.W. Till, S.J. Judd, B. McLoughlin, Reduction of faecal coliform bacteria in sewage effluents using a microporous polymeric membrane, Water Research 32 (1998) 1417–1422.
[37] I.-S. Chang, C.-H. Lee, Membrane filtration characteristics in membrane-coupled activated sludge systems—the effect of physiological states of activated sludge on membrane fouling, Desalination 120 (1998) 221–233.
[38] M. Gander, B. Jefferson, S. Judd, Aerobic MBRs for domestic wastewater treatment: a review with cost considerations, Separation and Purification Technology 18 (2000) 119–130.
[39] M. Mulder, Basic Principles of Membrane Technology, 2nd ed., Kluwer Academic Publishers, Dordrecht, 2003.